Lattice thermal conductivity reduction and phonon localizationlike behavior in superlattice structures

Rama Venkatasubramanian*
Research Triangle Institute, Research Triangle Park, North Carolina 27709
(Received 14 May 1999; revised manuscript received 10 August 1999)

A study of thermal conductivities perpendicular to the interfaces in Bi_2Te_3/Sb_2Te_3 superlattices is presented. The lattice thermal conductivities in these short-period superlattices are less than those in homogeneous solid-solution alloys and exhibit a minimum for a period of ~50 Å. For periods less than 50 Å, the adjoining layers of the superlattice apparently become coupled and, in effect, make their thermal conductivities approach that of an alloy. Using the mean free path from kinetic theory, a diffusive transport analysis suggests a low-frequency cutoff (ω_{cutoff}) in the spectrum of heat-conducting phonons. A physical model based on the coherent backscattering of phonon waves at the superlattice interfaces is outlined for the reduction of lattice thermal conductivity; this suggests conditions of localizationlike behavior for the low-frequency phonons. The ω_{cutoff} from the diffusive transport model is comparable to that estimated from applying the Anderson criterion to the potential localization of phonon waves. The general behavior of localizationlike effects is not unique to Bi_2Te_3/Sb_2Te_3 superlattices; it is also apparent in the thermal conductivities of Si/Ge superlattices. These superlattice structures offer a scope for studying the phonon localization phenomena while the lattice thermal conductivity reduction could lead to high-performance thermoelectric materials.

INTRODUCTION AND BACKGROUND

High figure-of-merit (Z) thermoelectric materials can enable efficient solid-state refrigeration and power conversion. The dominant state-of-the-art thermoelectric materials are based on solid-solution alloys in the $(Bi_xSb_{1-x})_2Te_3$ and $Bi_2(Se_yTe_{1-y})_3$ system or in the SiGe alloy system. The rationale for solid-solution alloying[1] is that the lattice thermal conductivity is reduced much more strongly than the electrical conductivity so that an overall enhancement in Z can be achieved for certain alloy compositions. Several of the approaches[2–4] being investigated to enhance the Z in thin-film thermoelectric materials would benefit from the reduced lattice thermal conductivity in low-dimensional structures. Utilizing this advantage, we have recently observed a factorial enhancement in Z with Bi_2Te_3/Sb_2Te_3 superlattices at 300 K, relative to state-of-the-art bulk alloy.[5]

Reduced thermal diffusivity[6] and controllable transmission characteristics of phonon waves[7] in superlattices had been reported prior to the first observation[8,9] of a significant reduction in the thermal conductivities, below those of solid-solution alloys, with superlattice structures. Also, the weaker carrier-phonon and phonon-phonon interactions, leading to slow decay of optically excited systems and slower dissipation of local Joule heating, respectively, have been documented in $Al_xGa_{1-x}As/GaAs$ superlattices relative to bulk GaAs.[10] Wave transport models predicting Bragg reflections at acoustic phonon frequencies have also been discussed.[7,11] It is not clear, however, if the transport behavior of long-wavelength heat-conducting phonons, diffusing under a local temperature gradient in a material, would be different from that observed for ''externally generated'' waves in the acoustic phonon frequency regime.[7,11]

Reliable data on thermal conductivities in superlattice structures, owing significantly to the thin-film thermal conductivity technique denoted as 3ω method developed by Cahill, Katiyar, and Abelson,[12] are just becoming available. Recent work[13] on the thermal transport properties of Si/Ge superlattices have confirmed the significant reduction in thermal conductivities. The benefits of such superlattice structures for advanced thermoelectrics have prompted detailed theoretical understanding of the thermal conductivities in superlattices using a Boltzmann transport model.[14,15] Several factors, including phonon dispersion relations and scattering at the superlattice interfaces, have been considered in the thermal transport models.[15] The various fitting parameters, to account for the different mechanisms, have yielded apparent agreement with experimental data. However, the general consensus is that the origin of the reduction of thermal conductivity in superlattice structures is not completely clear.

In this paper, for the first time to our knowledge, an attempt has been made to measure the lattice component of the cross-plane thermal conductivities in superlattice structures; the Bi_2Te_3/Sb_2Te_3 superlattice system[16] is presented as an example. We present the results of this study and indicate a model for the reduction of lattice thermal conductivity in superlattice structures. First, we present a phonon diffusive transport analysis that indicates a low-frequency cutoff (ω_{cutoff}) in the spectrum of phonons that transport heat. A physical model for the reduction of lattice thermal conductivity based on the coherent backscattering of phonon waves at the superlattice interfaces is outlined. We propose a localizationlike behavior depending on the frequency of phonons. It is similar to photon localization in highly scattering media, such as superlattices[17] and semiconductor powders;[18] this model is also consistent with the experimentally observed selective transmission of high-frequency phonons in superlattices.[7]

EXPERIMENT

The Bi_2Te_3/Sb_2Te_3 superlattices were grown on single-crystal, semi-insulating GaAs substrates by metallorganic

chemical vapor deposition.[16] Transmission electron microscopy[16] studies have revealed that these superlattices exhibit good interfacial quality even in the monolayer range (~10 Å). Carrier transport studies[16] and x-ray diffraction studies[19] have also indicated that these superlattices are of good quality for both short and large periods. We have carried out an extensive study, based on a large number of high-quality superlattice samples, of the variation of thermal conductivity with the superlattice period and free-carrier level. The superlattice periods investigated ranged from ~20 to ~180 Å. The free-carrier level in the *p*-type Bi_2Te_3/Sb_2Te_3 superlattice, for a given superlattice period, was typically varied from $\sim 8\times10^{18}$ to $\sim 2\times10^{19}\,cm^{-3}$. The superlattice layer thickness for the thermal conductivity measurement was in the range of 4000–7000 Å.

Cross-plane thermal conductivity measurement

The thin-film 3ω method[12] has been utilized for the measurement of thermal conductivities normal to the Bi_2Te_3/Sb_2Te_3 superlattice interfaces. Note that superlattice structures, by the very nature of their interfaces, are expected to exhibit anisotropic thermal conductivities. This is true even in materials that do not exhibit anisotropy in bulk form; this has been reported in $GaAs/Al_xGa_{1-x}As$ superlattices.[20] However, when heater widths are significantly larger than the film thicknesses, the thin-film 3ω method[12] is expected to measure the cross-plane thermal conductivities in superlattices.[13] Recently, we have also observed that the thermal conductivities measured by the 3ω method are comparable to those from the thermoreflectance technique, another independent cross-plane thermal conductivity measurement method, in Si/Ge superlattices. Additional results described below further validate that the thin-film 3ω method measures the cross-plane thermal conductivity in anisotropic structures.

Heater widths and superlattice film thickness were 10–20 μm and 0.4–0.6 μm, respectively, for the 3ω measurements. Pinhole-free dielectric isolation (Si_3N_4 of thicknesses ~0.06–0.1 μm) is needed to carry out the 3ω measurements on electrically conducting thin films. The through-thickness heat transport in the superlattice and Si_3N_4 films adds a frequency-independent component to the thermal response of the substrate.[12] We accounted for the thermal resistance of the Si_3N_4 dielectric isolation layer by carrying out a separate 3ω measurement on a reference GaAs substrate, also with the same thickness of the Si_3N_4 dielectric layer as in the superlattice. This procedure enables the experimental determination of ΔT_{osc} related to the substrate, as opposed to its theoretical estimation. From the ΔT_{osc} of the composite and that of the substrate, along with the power input per unit length, the thermal conductivity of the superlattice film can be determined.[12] The measurement can be cross-checked by being able to obtain accurately the thermal conductivity of the substrate from the slope of the ΔT_{osc} vs $\ln(2\omega)$ variation for the substrate+Si_3N_4+superlattice composite. This method was calibrated by measuring the properties of well-known films such as thermally grown oxides on Si.

The raw 3ω data (300 K) from a Bi_2Te_3/Sb_2Te_3 superlattice (SL) structure with the Si_3N_4 dielectric isolation for two heater widths are shown in Fig. 1. Here, the superlattice film thickness is ~0.44 μm. We observe very-well-behaved 3ω data, owing in significant measure to the excellent quality of the Si_3N_4 dielectric isolation layer. With the 10-μm heater, we obtain the thermal conductivity of the superlattice film (K_{SL}) as 0.535 ± 0.016 W/m K. For this set, the reference K_{GaAs} (without the superlattice film) was 46.5 ± 1.4 W/m K, while K_{GaAs} (with the superlattice film) was 45.1 ± 1.4 W/m K. With the 20-μm heater, K_{SL} was 0.509 ± 0.015 W/m K, while K_{GaAs} (without the superlattice film) was 44.8 ± 1.3 W/m K and K_{GaAs} (with the film) was 44.2 ± 1.3 W/m K. These measured K_{GaAs} values are excellent, close to its known value.[21] The observed near-independence of the measured K_{SL} with respect to the heater width used for the measurement and the accuracy in the extraction of K_{GaAs} (with the SL film) are attributable to the negligible role of any in-plane thermal spreading effects in the superlattice film. This, therefore, indicates the validity of a one-dimensional thermal transport through the thickness of the film.

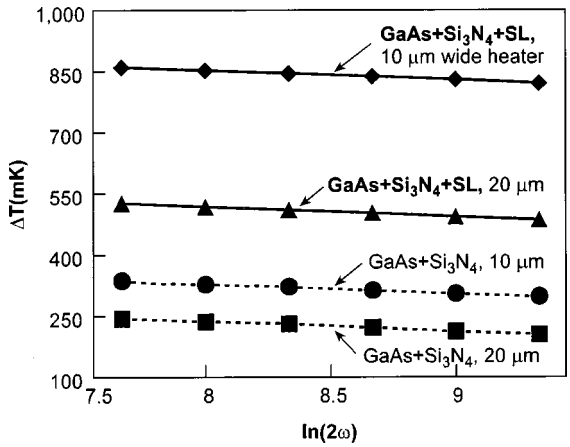

FIG. 1. ΔT vs $\ln(2\omega)$ for two heater widths, used for the elucidation of the cross-plane thermal conductivity measurement by the 3ω method in Bi_2Te_3/Sb_2Te_3 superlattices.

The ability of the 3ω method to determine the cross-plane thermal conductivity in the potentially anisotropic Bi_2Te_3/Sb_2Te_3 superlattices was further checked using a mesa geometry (following Ref. 22). The mesa structure ensures that the heat transport is one-dimensional through the superlattice interfaces. The thermal conductivities from the conventional and the mesa-etched thin-film structures were within 5% of each other. Noting that the ratio of heater width to film thickness is between 20 and 40 in our measurements, these results are similar to the modeling and experiments on the cross-plane thermal conductivity of anisotropic polymeric films.[22] Most importantly, the cross-plane thermal conductivities measured by the 3ω method in the Bi_2Te_3/Sb_2Te_3 superlattices were found to be in agreement with those obtained from through-thickness Peltier effect measurements in thin-film thermoelements processed with these superlattice films.[5]

3ω measurements between 300 and 150 K on a limited number of Bi_2Te_3/Sb_2Te_3 superlattice samples indicated the general behavior was comparable to that reported for Si/Ge superlattices.[13] In this paper, however, we focus on the 300-K thermal conductivities in the Bi_2Te_3/Sb_2Te_3 superlattices.

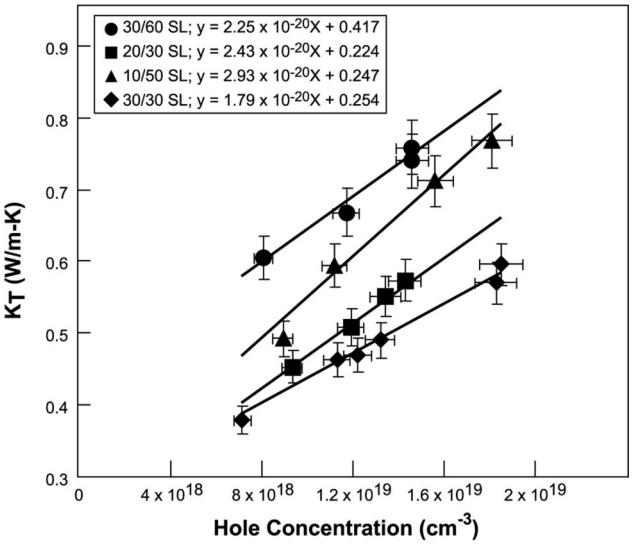

FIG. 2. Total thermal conductivity as a function of free-carrier concentration in some of the Bi_2Te_3/Sb_2Te_3 superlattice structures.

LATTICE THERMAL CONDUCTIVITY IN SUPERLATTICES

The 3ω method measures the total cross-plane thermal conductivity (K_T), consisting of the lattice component (K_L) and the electronic component (K_e). K_e is given by Eq. (1), where L_0 is the Wiedemann-Franz constant, q is the charge of the carrier, $\mu_\perp$ is the carrier mobility in the cross-plane direction, p is the carrier concentration, and T is the absolute temperature:

$$K_e = L_0 T(qp\mu_\perp). \tag{1}$$

K_L can be obtained from the y intercept in the plot of K_T as a function of p, if we assume that $\mu_\perp$ is nearly independent of carrier level. In these superlattices, the Hall-effect measurements indicate that the carrier mobilities are relatively independent (within 10%) for carrier levels in the range of 5×10^{18} to about $3.5\times10^{19}\,\mathrm{cm}^{-3}$.[16] This stems from weak ionized impurity scattering effects. For carrier transport perpendicular to the superlattice interfaces, any small reduction in carrier mobility from increased impurity scattering at higher carrier level is expected to be offset by a higher transport function across the potential barrier (even if only shallow in these superlattices); this can be understood from the movement of the Fermi level towards the valence-band edge with higher hole concentration. The linear behavior of the K_T-vs-p variation for the Bi_2Te_3/Sb_2Te_3 superlattice structures shown in Fig. 2 supports this argument.

We observe that the lattice thermal conductivities of the 10 Å/50 Å and the 30 Å/30 Å Bi_2Te_3/Sb_2Te_3 superlattices with the same period are the same, $\sim$0.25 W/m K. A similar study of K_T vs carrier conductivity gives a K_L of 0.49 W/m K for $Bi_xSb_{1-x}Te_3$ ($x\sim0.9\pm0.15$) alloy films along the c axis. For these alloy films we had to account for the relatively non-negligible mobility change with carrier concentration along the c axis, the direction of measured thermal conductivity. This K_L is in agreement with that of Rosi and Ransberg[23] for an alloy of similar composition as well as with that deduced from the data of Scherrer and Scherrer[24] for comparable alloys.

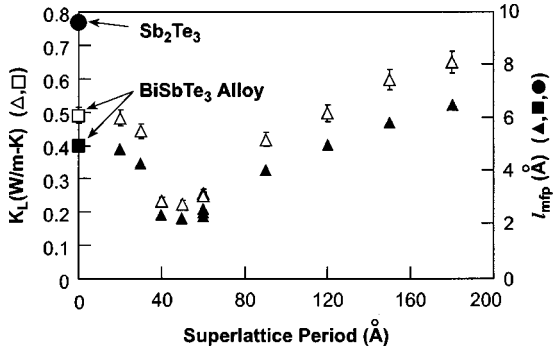

FIG. 3. Experimental lattice thermal conductivity (K_L) and calculated average phonon mean free path (l_{mfp}) as a function of the period in Bi_2Te_3/Sb_2Te_3 superlattices and other reference materials. Note: There are three data points, almost on top of each other, at the 60 Å period, corresponding to 30 Å/30 Å, 10 Å/50 Å, 20 Å/40 Å structures.

The variation of the lattice thermal conductivity (K_L) as a function of the superlattice period is shown in Fig. 3. Three points are worth noting: (1) The K_L of the superlattice structures shows a minimum for a period of $\sim$50 Å. The minimum K_L is $\sim$0.22 W/m K; this value is nearly a factor of 2.2 smaller than that obtained for a solid-solution alloy. (2) The K_L of larger-period superlattices exceed that of the solid-solution alloy but begin to approach that of a weighted average of Bi_2Te_3 ($K_L\sim1.05$ W/m K) and Sb_2Te_3 ($K_L\sim0.96$ W/m K). (3) For superlattice periods $<$50 Å, K_L begins to increase from the above minimum and starts approaching that of the solid-solution alloy. The variation of K_L and its approach to that of the alloy in ultrashort-period superlattices is similar to the reported behavior of total thermal conductivity in ultrashort superlattices.[9,25]

MEAN-FREE-PATH REDUCTION IN SUPERLATTICES

Kinetic theory[26] gives the average phonon mean free path (l_{mfp}) from

$$K_L = \tfrac{1}{3} c\rho\langle v_t\rangle l_{\mathrm{mfp}}, \tag{2}$$

where c is the specific heat, ρ is the density, and $\langle v_t\rangle$ is the average phonon velocity. Even in the presence of localizationlike effects, as observed later, this velocity can be thought of as the speed at which the energy is transported locally by wave diffusion in a ''viscous'' medium.[27]

The variation of l_{mfp} as a function of the superlattice period is also shown in Fig. 3; the behavior essentially resembles the variation of K_L, normalizing for the $c\rho$ product in the various superlattices. For the calculations of l_{mfp}, both c and ρ in a superlattice were assumed to be weighted averages of the individual layer components, Bi_2Te_3 and Sb_2Te_3. Note that the Debye temperatures of both these materials are $\sim$160 K,[28] much lower than the temperature of discussion (300 K). In addition, these materials have a rather large number of atoms per unit cell. Thus, the specific heat at 300 K would be dominated by the high-frequency acoustic and optical phonons due to the frequency dependence of density of states. This seems apparent including the effect of singularities in the phonon density of states from Born–von Kármán model.[28] Thus the specific heats of the constituents of the superlattice should be comparable to their bulk values, independent of the propagation (or lack of it) of the low-

frequency heat-conducting phonons for $T/\theta_{\text{Debye}} > 1$. We have used a $\langle v_t \rangle$ of $\sim 2.4 \times 10^5$ cm/sec in the estimation of l_{mfp} in the various superlattices, the alloy, and Sb_2Te_3 shown in Fig. 3. The closeness of the estimated $\langle v_t \rangle$ to the phase velocity (v_p) is due to the near-linear experimental dispersion curves in these materials (for most part of the longitudinal and transverse acoustic phonon spectra) along the trigonal axis. Certainly, more rigorous calculations of $\langle v_t \rangle$ are possible when localization effects are at work.[27]

We can consider the physical significance of the estimated l_{mfp} in the above materials. For example, in Sb_2Te_3 we estimate a l_{mfp} of ~9.6 Å from its K_L. The value of 9.6 Å is close to the repeat spacing of van der Waals bonding in the crystal. This bonding by its nature could potentially vary from layer to layer, thereby, creating a potential anharmonicity along the axis of heat flow. Similarly, for the $BiSbTe_3$ alloy film, we estimate a l_{mfp} of ~4.9 Å from its measured K_L. Remarkably, this is about the average separation between a Bi and a Sb atom in a lattice of the random alloy. For superlattices with the lowest K_L, we obtain a l_{mfp} of ~2.2 Å. We believe, in these superlattices, the region of anharmonicity could be in the vicinity of the van der Waals gap, due to the different covalent components (Bi_2Te_3 or Sb_2Te_3) on its either side.

DIFFUSIVE TRANSPORT ANALYSIS

From l_{mfp} and the effective diffusivity ($D \sim \frac{1}{3}\langle v_t \rangle l_{\text{mfp}}$) of phonons, we can obtain the spectrum of frequencies that potentially conduct heat. We start from the one-dimensional continuity relation[29] for the transport of heat to get the familiar diffusion equation. The frequency-domain solution to this problem is well known and provides an estimate for the range of the temperature wave[30] for a given angular frequency (ω) via

$$l = (2D/\omega)^{1/2}. \tag{3}$$

As the linear heat conduction by phonons would occur for a length scale $< l_{\text{mfp}}$ noting that for length scale $> l_{\text{mfp}}$ the phonons would have been scattered in another direction, we estimate that a given D and l_{mfp} would set a low-frequency cutoff, ω_{cutoff}, given by

$$\omega_{\text{cutoff}} = \tfrac{2}{3}\langle v_t \rangle (l_{\text{mfp}})^{-1}. \tag{4}$$

Thus the reduced l_{mfp} in superlattice structures (Fig. 3), compared to the solid-solution alloy, leads us to conclude that the low-frequency phonons would be inhibited from transport while the high-frequency phonons would be allowed to propagate in superlattices. This is in agreement with observation of a lossy transmission of low-frequency phonons and the near-complete transmission of the high-frequency phonons in $GaAs/Al_xGa_{1-x}As$ superlattices.[7] The calculated low-frequency cutoff as a function of the superlattice period for the Bi_2Te_3/Sb_2Te_3 superlattices is shown in Fig. 4.

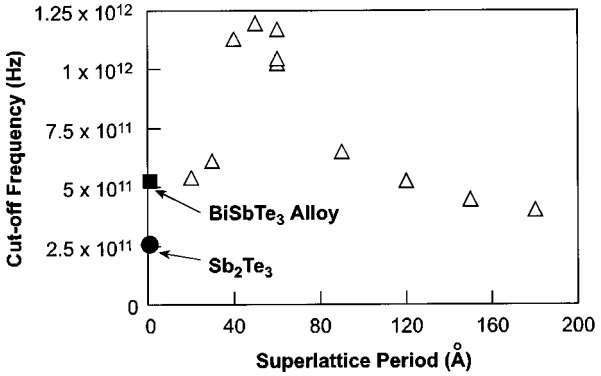

FIG. 4. Calculated low-frequency cutoff as a function of period in Bi_2Te_3/Sb_2Te_3 superlattices compared with that of an alloy and Sb_2Te_3.

PHONON REFLECTION AT SUPERLATTICE INTERFACES

Although we can relate the reduction in the average l_{mfp} to the blocking of low-frequency phonons, we need a physical model for the reduction of l_{mfp}. In other words, how does the anharmonicity, as indicated earlier, reduce the l_{mfp}? Here, we invoke the coherent backscattering of phonon waves at the superlattice interfaces, the regions of anharmonicity. This is similar to photon localization in highly scattering media.[17,18]

Let us consider a simple picture of a uniform alloy made of two components M_1 and M_2 and that of a superlattice consisting of two individual layers of M_1 and M_2 as shown in Fig. 5. The alloy would exhibit an average ''acoustic impedance'' Z_{av} that is related to the masses M_1 and M_2, as described by Brillouin.[31] In the superlattice, each of the two layers has a characteristic impedance Z_1 and Z_2, respectively. At first glance it would appear that the specific arrangements of atoms among the available lattice sites are irrelevant to the propagation of long-wavelength acoustic phonons. However, note that the acoustic mismatch would lead to reflection of the phonon waves at the interface.[31] Thus, in a superlattice, the *acoustic long-wavelength phonons not only ''see'' the varying composition (as much in the random alloy) but also experience reflection at the periodic interfaces*.

The reflection aspect in conjunction with a Bragg reflection model has been invoked by Narayanamurti *et al.*[7] They

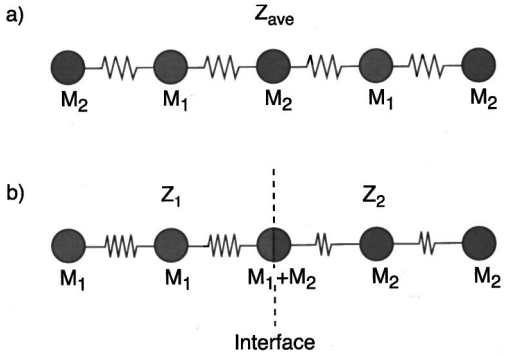

FIG. 5. Schematic of (a) an alloy and (b) a superlattice showing the potential for reflection of waves at the interface of a superlattice.

used the acoustic impedance mismatch model to indicate that the transmission should be minimized when the superlattice period is $\sim\lambda/2$, where λ is the phonon wavelength, in analogy with optical filters. However, in a subsequent paper Kelly[10] has indicated that the transmission should be a maximum when the phonon wavelength matches the superlattice period. Kelly[10] pointed out that the difference might be that inelastic processes are involved in the observations of Narayanamurti *et al.*[7]

However, the reflection of phonon waves can lead to an enhanced probability of a phonon wave coming back to its point of origin (in a local sense). This coherent backscattering is frequently referred to as weak localization or as a precursor to wave localization. In addition to backscattering, randomness is required to initiate a tendency for localization. A possibility in this regard is the varying amount of van der Waals bonding along the various superlattice interfaces, exemplified by the fluctuation in the electron diffraction intensity that we have observed within one of the bilayers of the superlattice.[16] We also note the strikingly nonlinear behavior of K_L versus the superlattice period (Fig. 3). Furthermore, larger-period samples are more opaque to phonon transport than smaller period samples, below the 50 Å scale, in Fig. 3. These observations suggest that localizationlike phenomena may be at work. We observe to our knowledge that such a localization aspect has not been invoked before to explain the thermal conductivity reduction in superlattices. The localization model may be appropriate in dealing with potential reflection of diffusing waves.[17,27] The backscattering should lead to a ''viscous'' medium[27] for phonon waves in the superlattice structures, over and above that attainable in solid-solution alloys. For one to observe the effects of such backscattering, of course, the superlattice interfaces probably have to be of high quality. The transmission electron microscopy studies and in-plane electrical transport data of the Bi_2Te_3/Sb_2Te_3 superlattices[16] do indicate that the superlattices under consideration are of good quality. Besides, the layered chlcogenides (such as Bi_2Te_3 and Sb_2Te_3), due to the van der Waals gap along the growth axis, are purported to be ideal materials[32,33] for obtaining ultrasharp interfaces in their respective heterostructures with very few interface defects.

EQUIVALENCE BETWEEN DIFFUSIVE TRANSPORT AND LOCALIZATION

In this section we discuss the equivalence between the diffusive transport analysis and the localizationlike behavior that can stem from back scattering at the superlattice interfaces. The Anderson localization phenomena can be inferred from a calculation of the kl_{mfp} product,[27] where k is the wave vector. From l_{mfp} and the phase velocity (v_p), we can estimate the kl_{mfp} product over the entire range of the acoustic phonon spectrum. The calculated kl_{mfp} products for some of the structures under discussion are shown in Fig. 6. We observe that in the short-period superlattices, the condition of $kl_{\mathrm{mfp}}<1$ is strongly met for a larger range of low frequencies, predicting localizationlike behavior. The cutoff frequency estimated for the various structures in Fig. 6 from the application of the Anderson localization criterion are comparable to those estimated from the diffusive transport model (shown in Fig. 4). This is not surprising since from Eq. (4)

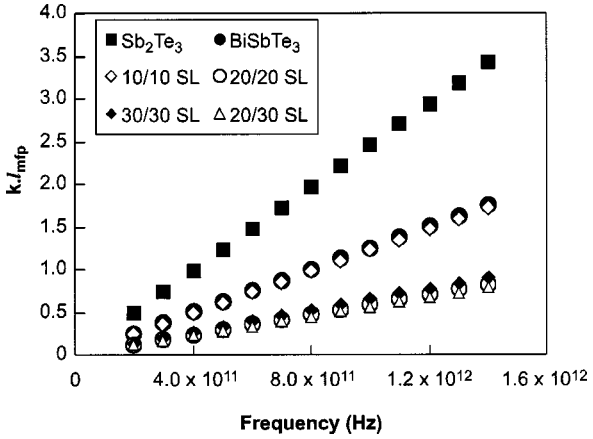

FIG. 6. Calculated kl_{mfp} product for some of the superlattices, alloy, and Sb_2Te_3 over the range of the acoustic phonon spectrum.

and from the fact that k_{cutoff} $(2\pi/\lambda_{\mathrm{cutoff}})$, we obtain relation (5); this can be compared with the Anderson localization criterion of $kl_{\mathrm{mfp}}\sim 1$ and the Ioffe-Riegel criterion[27] of $0.5 < kl_{\mathrm{mfp}} < 0.985$:

$$k_{\mathrm{cutoff}} l_{\mathrm{mfp}} = \tfrac{2}{3}(\langle v_t \rangle / v_p). \tag{5}$$

APPARENT RISE IN K_L AND l_{mfp} OF ULTRASHORT-PERIOD SUPERLATTICES

We can now consider the rise in K_L and the l_{mfp} (Fig. 3) in ultrashort-period superlattices (period <50 Å). This discussion is only intended to be qualitative and needs a more detailed quantitative modeling. First, we observe that it is tempting to attribute this behavior to phonon-tunneling effects, given the near-exponential rise in thermal conductivity (Fig. 3) with $(\mathrm{period})^{-1}$. However, we discount this possibility, as the 10 Å/50 Å, 20 Å/40 Å, and 30 Å/30 Å superlattices (all with a period $\sim$60 Å) show nearly the same K_L and about similar mean free paths (Fig. 3). Thus, if phonon tunneling through a 10-Å region were dominant in order to explain the difference between the 10 Å/10 Å and the 30 Å/30 Å superlattice, then one would expect the K_L of the 10 Å/50 Å superlattice to be markedly different from that of a 30 Å/30 Å superlattice. However, this is not the case.

The behavior of ultrashort-period superlattices can be understood if we compute the wavelengths using the phase velocity for the cutoff frequencies shown in Fig. 4. The cutoff wavelength ($\lambda_{\mathrm{cutoff}}$) is plotted as a function of the superlattice period in Fig. 7(a). We observe that near the point where the minimum lattice thermal conductivity (equivalent to minimum average phonon transmission) is approached, the superlattice period is $\sim 2\lambda_{\mathrm{cutoff}}$. Under this condition, we can consider a schematic of the phonon waves, for the critical frequency, in the two individual layers of the superlattice as shown in Fig. 7(b) for $d_{\mathrm{Bi_2Te_3}} \sim d_{\mathrm{Sb_2Te_3}}$. When the cutoff wavelengths calculated by the diffusive transport analysis start approaching and exceeding the individual layer thicknesses in *both* layers, the two layers probably become coupled and so the effect of acoustic mismatch starts to disappear. From this viewpoint, the cutoff wavelength would not decrease any further with the reduction of the superlattice

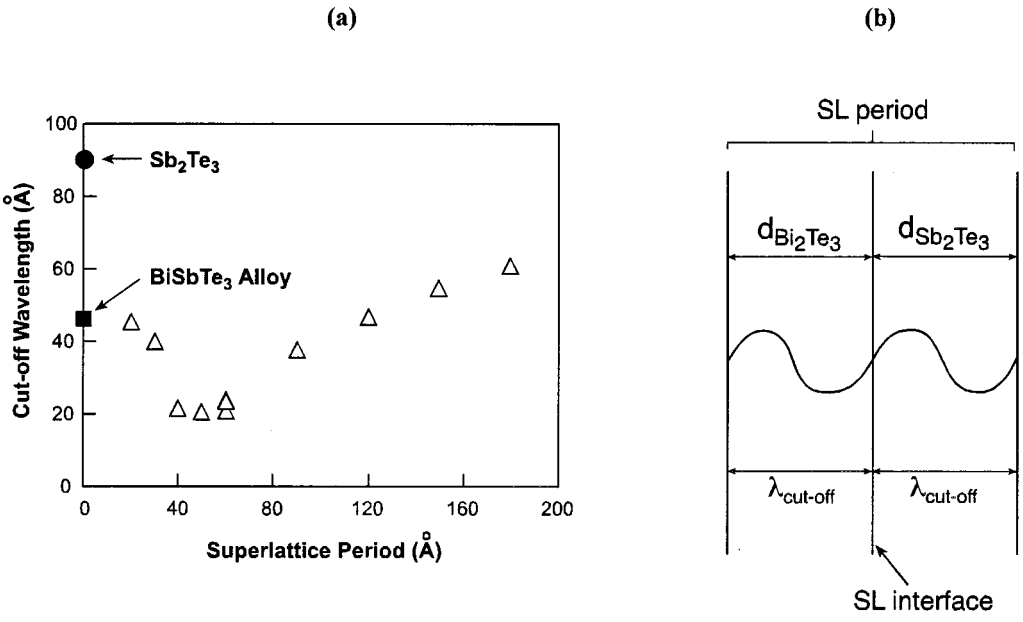

FIG. 7. (a) Low-frequency cutoff wavelength as a function of superlattice period and (b) the approximate situation when the superlattice period $\sim 2\lambda_{\text{cutoff}}$.

period and the long-wavelength phonons would begin to be transported across the interfaces. It is interesting to observe that the condition for *maximum* transmission as per Kelley[10] is at a period $\sim\lambda$ and we indicate *minimum* transmission at a period $\sim 2\lambda_{\text{cutoff}}$.

CONCLUDING REMARKS

The general behavior of lattice thermal conductivity in superlattices, with a minimum around certain intermediate periods, is not unique to the Bi_2Te_3/Sb_2Te_3 superlattices. The *in-plane* lattice thermal conductivities in Si/Ge superlattices as a function of their period indicate a similar behavior.[34] We have observed a rather sharp minimum for superlattice periods of 65–75 Å at 300 K. A realistic modeling of this data is complicated by the fact that the θ_{Debye} of these materials (450–600 K) is significantly larger than the temperature of measurement. Also, the in-plane heat transport, especially in such periodic structures, may have to be effectively treated as a three-dimensional problem. Even so, our preliminary calculations suggest that phonon-reflection effects leading to a localizationlike behavior may be at work in this system as well for superlattice periods of 65–75 Å. In conclusion, the heat transport in superlattice structures may offer a scope for understanding the potential effects related to phonon localization phenomena. Most importantly, however, the lattice thermal conductivity reduction offered by the superlattices may be very useful to obtaining high-performance thermoelectric materials.[5,34]

ACKNOWLEDGMENTS

Dr. S. Wolf at Defense Advanced Research Projects Agency and Dr. J. Pazik at the Office of Naval Research are acknowledged for the support of this work. The author is grateful the support of Dr. K. Stokes in the 3ω measurement setup and the technical assistance of T. Colpitts and E. Siivola. The collaboration with the Thermal Sciences Group of Professor K. Goodson of Stanford University and the comments of Dr. M. Stroscio of the Army Research Office, Research Triangle Park, NC, are acknowledged.

*Electronic address: rama@rti.org

[1] D. A. Wright, Nature (London) **181**, 834 (1958).
[2] L. D. Hicks and M. S. Dresselhaus, Phys. Rev. B **47**, 12 727 (1993).
[3] R. Venkatasubramanian and T. S. Colpitts, in *Thermoelectric Materials—New Directions and Approaches*, edited by T. M. Tritt *et al.*, MRS Symposia Proceedings No. 478 (Materials Research Society, Pittsburgh, 1997), p. 73.
[4] G. D. Mahan and L. M. Woods, Phys. Rev. Lett. **80**, 4016 (1998).
[5] R. Venkatasubramanian, E. Siivola, T. Colpitts, and B. C. O'Quinn, in Proceedings of the 18th International Conference on Thermoelectrics, Baltimore (IEEE, New York, in press).
[6] T. Yao, Appl. Phys. Lett. **51**, 1798 (1987).
[7] V. Narayanamurti, H. L. Störmer, M. A. Chin, A. C. Gossard, and W. Wiegmann, Phys. Rev. Lett. **43**, 2012 (1979).
[8] W. S. Capinski and H. J. Maris, Bull. Am. Phys. Soc. **41**, 692 (1996); See also Physica B **219&220**, 699 (1996).
[9] R. Venkatasubramanian, Bull. Am. Phys. Soc. **41**, 693 (1996); See also Nav. Res. Rev. **48** (4), 31 (1996).
[10] M. J. Kelly, J. Phys. C **18**, 5963 (1985).
[11] S. Tamura, D. C. Hurley, and J. P. Wolfe, Phys. Rev. B **38**, 1427 (1988).
[12] D. G. Cahill, M. Katiyar, and J. R. Abelson, Phys. Rev. B **50**, 6077 (1994).
[13] S.-M. Lee, D. G. Cahill, and R. Venkatasubramanian, Appl. Phys. Lett. **70**, 2957 (1997).
[14] P. Hyldgaard and G. D. Mahan, Phys. Rev. B **56**, 10 754 (1997).
[15] G. Chen, Phys. Rev. B **57**, 14 958 (1998).
[16] R. Venkatasubramanian, T. Colpitts, B. C. O'Quinn, S. Liu, N. El-Masry, and M. Lamvik, Appl. Phys. Lett. **75**, 1104 (1999).

[17] S. John, Phys. Rev. Lett. **58**, 2486 (1987).
[18] D. S. Wiersma, P. Bartolini, A. Lagendijk, and R. Righini, Nature (London) **390**, 671 (1997).
[19] R. Venkatasubramanian, T. Colpitts, N. El-Masry, and M. Lamvik, J. Cryst. Growth **170**, 817 (1997).
[20] G. Chen, C. L. Tien, X. Wu, and J. S. Smith, J. Heat Transfer **116**, 325 (1994).
[21] S. M. Sze, *Physics of Semiconductor Devices* (Wiley, New York, 1981).
[22] Y. S. Ju, K. Kurabayashi, and K. Goodson, Thin Solid Films **339**, 160 (1999).
[23] F. D. Rosi and E. G. Ransberg, in *Thermoelectricity*, edited by P. H. Egli (Wiley, New York, 1960).
[24] H. Scherrer and S. Scherrer, in *CRC Handbook of Thermoelectrics*, edited by D. M. Rowe (CRC, New York, 1995), p. 211.
[25] I. Yamasaki, R. Yamanaka, M. Mikami, H. Sonobe, Y. Mori, and T. Sasaki, in *Proceedings of the 17th International Conference on Thermoelectrics* (IEEE, New York, 1998), p. 211.
[26] C. Kittel, *Introduction to Solid State Physics* (Wiley, New York, 1976).
[27] P. Sheng, *Introduction to Wave Scattering, Localization, and Mesoscopic Phenomena* (Academic, London, 1995).
[28] A. Krost, *Numerical Data and Functional Relationships in Science and Technology*, Landolt-Börnstein, New Series, Group 3, Vol. 17, edited by O. Madelung, M. Schulz, and H. Weiss (Springer-Verlag, Berlin, 1983).
[29] H. S. Carslaw and J. C. Jaeger, *Conduction of Heat in Solids* (Oxford University Press, Oxford, 1959).
[30] K. Seeger, *Semiconductor Physics* (Springer-Verlag, Heidelberg, 1982).
[31] L. Brillouin, *Wave Propagation in Periodic Structures* (McGraw-Hill, New York, 1946).
[32] O. Lang, R. Schalf, Y. Tomm, C. Pettenkofer, and W. Jagermann, J. Appl. Phys. **75**, 7805 (1994).
[33] A. Koma, Thin Solid Films **216**, 72 (1992).
[34] R. Venkatasubramanian, E. Siivola, and T. Colpitts, in *Proceedings of 17th International Conference on Thermoelectrics* (Ref. 25), p. 191.